Topology optimization considering the requirements of deep-drawn sheet metals

Robert Dienemann[1], Axel Schumacher[2], Sierk Fiebig[3]

[1,2] University of Wuppertal, Faculty D – Mechanical Engineering, Chair for Optimization of Mechanical Structures,
Wuppertal, Germany
[1] dienemann@uni-wuppertal.de
[2] schumacher@uni-wuppertal.de
[3] Volkswagen AG, Braunschweig, Germany, sierk.fiebig@volkswagen.de

1. Abstract

Topology-optimized designs for minimum compliance or minimum stress at minimum mass are often framework structures due to their homogeneous stress distribution over the cross section and therefore the best possible material utilization. From the manufacturing's point of view complex framework structures, which often develops during topology optimization, are difficult to manufacture because of possible undercuts. Manufacturing of these designs is often only possible by joining of numerous components or by 3D printing.

For mass production sheet metal parts manufactured by deep drawing are often more efficient concerning the costs in relation to their performance. Therefore we implemented a manufacturing constraint to the 3D topology optimization based on the density method ensuring that thin walled structure results. Thereby more flexibility for the mid surface design and also for cut-outs is reached compared to the optimization based on CAD-parameters. Also a variable thickness distribution for tailored blanks can be achieved.

Results for deep drawing structures with optimized topologies will be compared with optimized structures without manufacturing restriction due to their performance.

2. Keywords: topology optimization, sheet metals, deep drawing, manufacturing constraint, thin walled structures

3. Introduction

The optimization of shell structures is important in the field of mechanical engineering, but also in civil engineering and architecture (roof structures). In these fields a strengthened research has taken place in recent years.

Ansola et. al [1] propose a combination of CAD-parameters for the mid surface description and the SIMP-algorithm for the identification of optimal cut-outs. Thereby the optimization algorithm runs serially through the shape optimization of the mid surface and afterwards the topology optimization. This approach was taken up by Hassani et al. [2] and a simultaneous shape- and topology-optimization was introduced. The shape optimization takes place in the Finite Element Model, which shape can be modified by control points of splines. Both methods highly depend on the parametrization of the mid surface.

Zienkiewicz and Campbell [3] use the node coordinates as design variables instead of the CAD-parameters. Thereby a larger freedom of design is achieved. However by using sensitivities of coordinates of boundary nodes the finite element mesh becomes irregular. Yonekura et al. [4] keep the mesh regularity for small shape modifications.

In literature there are few attempts for the optimization of shells based on solid elements. Lochner-Aldinger and Schumacher [5] use the density method and extract isosurfaces of the element densities as mid surfaces.

4. The new approach for topology optimization for deep-drawn sheet metals

Our new approach uses the homogenisation method [6] on a linear voxel mesh. The derived method *Solid Isotropic Material with Penalisation* (SIMP) introduces material with the artificial density $0 < \rho_i \leq 1$ and Young's modulus E_i in element i (see equation 1). E_0 is the Young's modulus of the basic material. By increasing the penalty exponent s over 1.0 intermediate densities are penalized and thereby the optimized design rather converges to a black&white design.

$$E_i = \rho_i^{\,s} E_0 \tag{1}$$

Because of the use of sensitivities our approach is suitable for linear static load cases. All kinds of objective functions or constraints can be used, if their sensitivities are known.

4.1. Calculation of the mid surface

To allow the manufacturing by deep drawing in a single forming step, the optimized structure must have
- no undercuts.
- a constant wall thickness. Thereby the thinning during the forming process is neglected. By not considering the forming process also the material hardening and residual stresses are ignored.

These two manufacturing constraints can be achieved by modifying the sensitivities of the objective function. An increase of the element densities is only allowed near the current mid surface. Thus the mid surface can move according to the sensitivities. The mid surface can be found by calculating the average of the element coordinates in the punch direction weighted with the element densities. Figure 1 shows the procedure of deriving the mid surface from the volume mesh. Only a single cross section is displayed. Initially the user has to define the global punch direction. The mesh is divided into columns with the same width w, which is the element edge length. The midpoint of each column is calculated by equation 2.
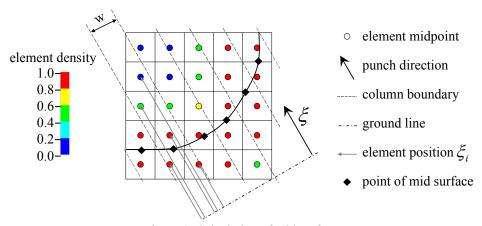

Figure 1: Calculation of mid surface

$$\xi_m = \frac{\sum \xi_i \cdot \rho_i}{\sum \rho_i} \tag{2}$$

ξ_i are the distances between the element midpoints from a ground line. For one exemplary column these distances are marked as grey arrows. The midpoint of each element decides to which column the element belongs. The connection of all midpoints with distance ξ_m present the mid surface.

4.2 Penalization of sensitivities

In order to get a shell structure sensitivities far away from the mid surface are penalized. The penalization factor P_i for the sensitivities of each element is calculated by equation 3.

$$P_i = \frac{1}{2}\left[1 - \frac{2}{\pi}\operatorname{atan}\left(\frac{a}{b}\left[d_i - \frac{b}{2}\right]\right)\right] \tag{3}$$

d_i is the minimum distances between the midpoint of element i and the mid surface. b is the user defined desired wall thickness, a/b describes the discreteness of the penalty function (see Figure 2). A larger quotient a/b ensures that the shell thickness does not exceed b, but slows down the convergence rate. The penalisation factor is normalized $P_i \in \left]0,1\right[$.
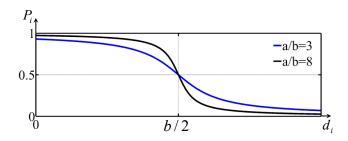
Figure 2: Graph of penalisation function for element sensitivities as a function of the distance from the mid surface

4.3. Convergence

The movement of the mid surface can stagnate, if the penalisation of the sensitivities is stronger than the improvement of the objective function. This problem is solved by alternating the desired wall thickness b. By increasing the desired wall thickness, elements are accumulated at the side of the shell, where the sensitivities are larger, by decreasing the desired wall thickness the shell's midface has moved to an improved design.

Also the penalisation of intermediate densities has an influence on the convergence. Figure 3 shows the movement of the mid surface. Only a single cross section is displayed. Even if a lower located mid surface would be better for the possible objective function compliance, the stiffness of the structure would temporarily decrease due to the lower stiffness of elements with penalized intermediate density (image at the right). That is the reason why the optimization starts without penalisation of intermediate densities (penalty exponent $s = 1$) until a convergence criterion is reached. Thereby at least the tensile/compressive stiffness remains the same between the images on the left and the right. After the increase of the penalty exponent this convergence problem is also solved by alternating the desired wall thickness.
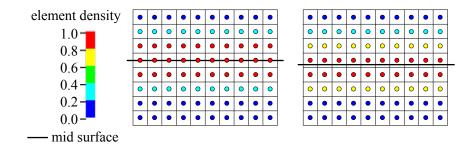

Figure 3: Movement of mid surface through change of elements densities

4.4 Optimization procedure

Figure 4 shows the optimization algorithm. Convergence criterion 1 can be the change of the objective function from one iteration to the next one or the maximum change of element densities. Convergence criterion 2 is the improvement of the objective function after the alternation of the desired wall thickness. During the alternation of the desired wall thickness and at the start of the optimization, the current desired wall thickness b_{curr} is larger than the desired wall thickness b.

5. Examples

In the following example topology optimizations of a cantilever beam (see Figure 5a) with and without manufacturing constraint are performed. The compliance is minimized considering a volume fraction constraint of 6.25 %. The design space is discretised by $120 \times 80 \times 48$ elements. One end of the structure is fixed, at one edge a line load of 200 N/mm is applied. The elements at the line load are defined as non-design space. A sensitivity filter with the radius of $r = (1.7 \text{ element edge lengths})$ and a penalty exponent $s = 3$ are used. The material is steel with Young's Modulus $E_0 = 210000 MPa$ and Poisson's Ratio $v = 0.3$.
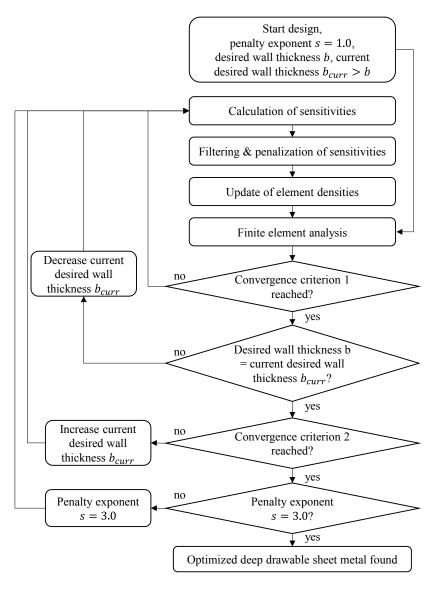
Figure 4: Optimization procedure

5.1 Cantilever Beam without manufacturing constraint

Without the manufacturing constraint a compliance of 32181.7 Nmm is achieved (see Figure 5b/c). 416 iterations were necessary followed by a final conversion to a black&white design. The convergence criterion is the improvement of the objective function per iteration of less than 0.01 % per iteration.
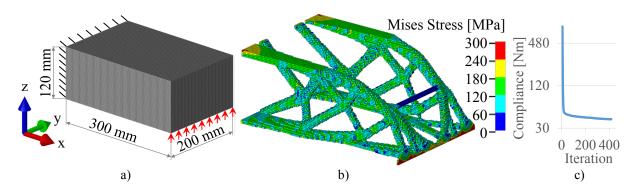

Figure 5: Cantilever Beam: a) FE-Model with loads and boundary condition, b) Stresses of final design (converted to black&white design) without manufacturing constraint, c) Compliance history

5.2 Cantilever Beam with manufacturing constraint

The same optimization task as in chapter 5.1 is performed by using the optimization procedure for thin walled structures described in chapter 4.4. The desired wall thickness is $b = (3 \text{ element edge lengths})$. This is the thinnest possible structure that ensures that a bending stress state can be represented with linear volume elements. The punch direction was chosen as z. The convergence criteria 1 and 2 were the improvement of the objective function per iteration of less than 0.1 %. The penalisation parameter for the manufacturing restriction is chosen as $a = 25$. Figure 6a shows the compliance history of the topology optimization process. In Figure 6b) the success of the alternation of the desired wall thickness between intermediate result [3] and [4] can be seen. In Figure 7 the design changes during the optimization process are shown.
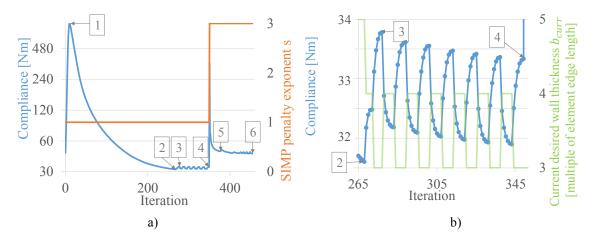

Figure 6: Compliance history: a) whole Optimization (logarithmic scale) with change of penalty exponent s, b) detail of convergence history with change of desired wall thickness
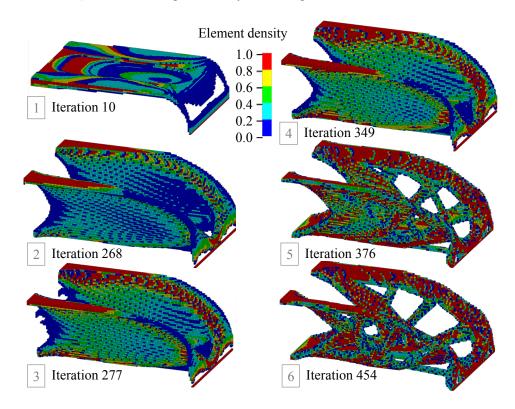

Figure 7: Element densities of intermediate results during the optimization (elements with density $x_i > 0.1$)

In Figure 8a the final black&white design of the shell structure is shown. This structure reaches a compliance of 40121.4 Nmm at a buckling safety of 5.98. In comparison to the optimization without manufacturing constraint the compliance is 24.7 % worse, whereby the manufacturing is much easier.

a)   b)
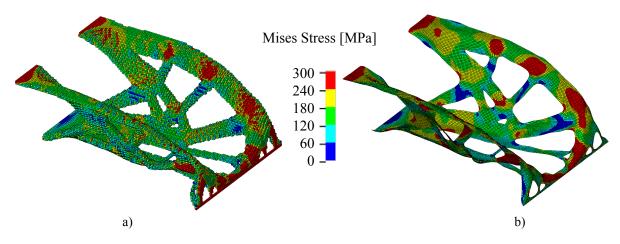
Figure 8: Stress a) of final design with manufacturing constraint (converted to black&white design), b) converted to surface model with shell elements

In order to check the quality of the finite element model with solid elements, a surface model of the optimized design with the same volume has been created. Thereby the compliance increases by 1.6 %. As to be seen in Figure 8, also the stresses are very similar, although the solid model is calculated with only three linear voxels across the sheet metal thickness.

6. Final remarks

Besides the shown application examples, the manufacturing constraint for the topology optimization of deep drawable sheet metals has been tested for several structures with multiple load cases. The results are promising, but we have to note that the gradient based optimization method will find most probably only local optima.

Compared to gradient based topology optimizations without manufacturing constraint the presented method needs more iterations and the objective function of the optimized designs is usually worse, but it can be guaranteed that the structures can be manufactured easily.

Further research activities will focus on the improvement of the computational efficiency, multishell structures, stress- and buckling constraints, the implementation of the deep drawing simulation in the optimization and automatization of the conversion to a surface model in order to perform a following shape optimization.

7. References

[1] R. Ansola, J. Canales, J.A. Tarrago and J. Rasmussen, On simultaneous shape and material layout optimization of shell structures, *Structural and Multidisciplinary Optimization*, 24, 175-184, 2002.
[2] B. Hassani, S.M. Tavakkoli and H. Ghasemnejad, Simultaneous shape and topology optimization of shell structures, *Structural and Multidisciplinary Optimization*, 48, 221-233, 2013.
[3] O.C. Zienkiewicz and J.S. Campbell, Shape Optimization and sequential linear programming, In: R.H. Gallagher and O.C. Zienkiewicz, *Optimum Structural Design*, John Wiley & Sons, Chichester, 1973.
[4] M. Yonekura, M. Shimoda and Y. Liu, Optimal Free-form Design of Shell Structure for Stress Minimization, *10th World Congress on Structural and Multidisciplinary Optimization*, Orlando, USA, 2013.
[5] I. Lochner-Aldinger and A. Schumacher, Homogenization method, In: S. Adriaenssens, P. Block, D. Veenendaal, C. Williams, *Shell Structures for Architecture – Form Finding and Optimization*, Routledge, New York, 2014
[6] M.P. Bendsøe, Optimal shape design as a material distribution problem, *Structural Optimization*, 1, 193-202, 1989